*Mining of Mineral Deposits*
*Volume 16 (2022), Issue 4, 47-55*

JOURNAL / MINING.IN.UA

https://doi.org/10.33271/mining16.04.047

# Analytical and numerical study of one-dimensional and two-dimensional stress distribution within an elastic semi-infinite material under the action of an arbitrary rectangular uniform loading

Farid Sh. Maleki[1*], Hamid Chakeri[2], Sajjad Chehreghani[3], Hossein Azad Soula[2]

[1] *University of Tehran, Tehran, Iran*
[2] *Sahand University of Technology, Tabriz, Iran*
[3] *Urmia University, Urmia, Iran*

**Corresponding author: e-mail s.chehreghani@urmia.ac.ir*

**Abstract**

**Purpose.** The study of stress distribution within an elastic semi-infinite material under the action of an external loading is of great importance in the theory of elasticity. In most cases, the lack of knowledge about the stress distribution within a material can result in incomplete and inappropriate engineering designs, leading to unsatisfactory consequences. The latter include cracks and fractures, created inside the concrete segmental lining in TBM tunneling, as well as indentations that occur in floors due to the lack of pillar design not only in underground mining, but even in civil projects. This study focuses on the one-dimensional and two-dimensional internal stress distribution induced by arbitrary rectangular–square loading, in other words, that applied to an elastic semi-infinite material.

**Methods.** Firstly, this paper uses an analytical method and, subsequently, a numerical method. In the analytical study, the point load equations of Boussinesq and Westergaard are used. Extending these equations to the rectangular loading area, four new equations are introduced. Using the Abaqus finite element software, the numerical study is performed in 3D space.

**Findings.** The results show that the answers from the introduced equations are in high consistency with numerical ones. However, the result of the extended Boussinesq point load equation is closer to the answer obtained by the numerical method.

**Originality.** Four new equations, presented in this paper, describe one-dimensional and two-dimensional stress distribution.

**Practical implications.** The presented equations can provide a simple and convenient way to solve rectangular load problems in many cases such as foundation, civil and mining projects. This study uses initial information on specific segments in the Tabriz Metro line-2 Project.

***Keywords:*** *stress distribution, rectangle, semi-infinite, Boussinesq, Westergaard*

## Nomenclature

$f_c$ – 28-day uniaxial compressive strength of the concrete segment;
$E_c$ – Young's modulus of concrete segment;
$\upsilon_c$ – the Poisson ratio of the concrete segment;
$\rho_c$ – the density of the concrete segment;
$f_r$ – Rupture modulus of concrete segment;
$f_t$ – Tensile strength of concrete segment;
$c_1$, $c_2$ – coefficients depended on the concrete;
$\delta$ – crack instantaneous opening in the concrete;
$\delta_0$ – crack ultimate opening in the concrete;
$\eta_c$ – the coefficient depended on the $\upsilon_c$;
$x$, $y$, $z$ – global coordinates;
$x_i$, $y_i$, $z_i$ – local coordinates;
$X$, $Y$ – the difference between global and local coordinates;
$P_o$ – the point load applied to the center of the loading area considering the global coordinates;
$P_i$ – the point load applied to any point of the loading area considering the local coordinates;
$\sigma_{z0}$ – the stress created within the segment along the $z$-axis due to $P_0$;
$\sigma_{zi}$ – the stress created within the segment along the $z$-axis due to $P_i$;
$\sigma_z$ – the stress created within the segment along the $z$-axis due to a rectangular loading;
$a$ – the arbitrary rectangle length;
$b$ – the arbitrary rectangle width;
$K$ – influence factor.

## 1. Introduction

It is well understood that any type of loading on a medium lead to the distribution of stress inside it. Knowledge of this distribution can help to predict the behavior of the material, being under loading, that can be used for future studies and design assumptions in engineering. The aim of this study is to provide a convenient method of stress distribution calculation within a material that is usable in wide range of engi-

Received: 4 September 2022. Accepted: 2 November 2022. Available online: 30 December 2022


Mining of Mineral Deposits. ISSN 2415-3443 (Online) | ISSN 2415-3435 (Print)

neering structures in mining, rock mechanics, geotechnics, and civil. The first solution to the problem of a pure vertical load located on a body was presented by Lame and Clapeyron that uses Fourier theory [1]. Boussinesq presented various potential functions to solve the problems of applying load on an elastic material including direct, inverse, and three-variable logarithmic potentials [2]. Love presented the stresses and dislocations caused by loading on rectangular and circular plates on a 3D semi-infinite object by generalizing the logarithmic potential of Boussinesq and the function of Newton's surface distribution potential [3]. Loading on a rectangular plate resulted in introducing the strip loading. Many writers have come up with ideas of the vertical load applied on a solid object by integrating Green's functions. In this regard, Lamb presented a new method, in which Terazawa solved the distributive vertical load problem by generalizing the method proposed by Lamb in the form of a Bessel-Fourier extension for circular loading [4].

Another method is the two-dimensional Airy stress function ($\varphi$). In this method, it is possible to solve the problem of stress distribution by taking into account the Cartesian or Polar polynomials presented in the theory of elasticity. So that a semi-infinite plane with a free surface of $z = 0$ is assumed [5].

It is well understood that many methods have been proposed to provide a solution for the rectangular uniform loading. Newmark has derived an expression for the vertical stress at a point below the corner of the loaded area [6]. Based on this equation, Fadum has prepared a chart for the influence values [7]. Steinbrenner has given another form of the chart for this purpose [8].

In this paper, the stress distribution within a semi-infinite material due to an arbitrary rectangular uniform loading has been discussed. Firstly, the analytical method has been used which provides a direct and accurate answer for this purpose. To do so, the Boussinesq and Westergaard point loading equations were generalized to a rectangular loading area in order to provide a closed form solution. In the presented method, there is no need to use any chart or any approximating method. Secondly, the numerical method has been adopted to verify the analytical investigation. Finally, Matlab codes have been generated to reduce the problem-solving time and simultaneously present an exact answer by providing a counterplot, illustrating the distribution of stress concentration due to an arbitrary rectangular uniform loading. The newly presented equations can be useful in a vast range of applications in engineering. For instance, in room and pillar underground mining, it is important to prevent the failure of the pillars and their indentation on the floor. Calculating the provided stress distribution and concentration due to the aforementioned pillars can help to design their critical cross-section. Also, these equations are applicable in constructing structures on the jointed slippery benches in open-pit mining to calculate the amount of stress applied to these defections to prevent failure. The mentioned equations can be utilized in the calculation of stress distribution inside the concrete segmental lining due to the hydraulic jacks' loading in EPB TBMs as well.

## 2. Analytical method

The analytical method was carried out to calculate the stress distribution mathematically within an elastic semi-infinite material under a rectangular uniform loading. This study was conducted in two ways encompasses one-dimensional (on the *z*-direction only) and two-dimensional (on the *xoz* plane) (Fig. 1). In this regard, point loading equations of Boussinesq and Westergaard were considered to be extended to a rectangular loading area to achieve the target. In one-dimensional stress distribution analysis, which is shown in Figure 1a, the amount of stress that occurred at the points located on the z-axis and its variation along the *z*-direction, perpendicular to the loading face, is under discussion. In two-dimensional stress distribution analysis, the amount of stress created at the points located on the *xoz* plane perpendicular to the loading face is studied (Fig. 1b). According to Figure 1, an arbitrary rectangle with dimensions of 2a × 2b was assumed as the loading face in this study.

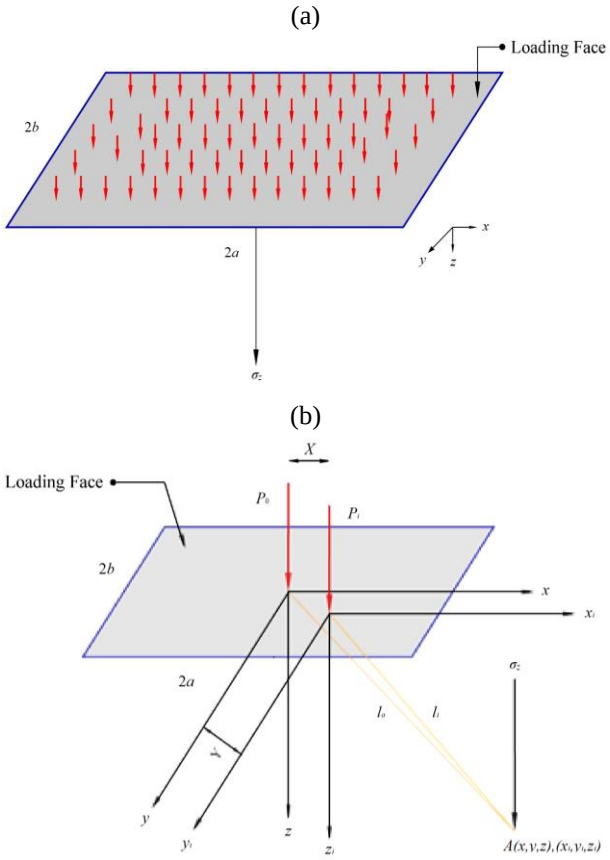


***Figure 1. Schematic of rectangular uniform loading (a) one-dimensional stress distribution; (b) assumptions of extending point load to the rectangular loading area in two-dimensional space***

Problem assumptions:

a) a global Cartesian coordinate system of ($x$, $y$, $z$) is considered;

b) a local Cartesian coordinate system of ($x_i$, $y_i$, $z_i$) is considered for each one of the point loads ($i = 1 \ldots n$);

c) the relationship between two Cartesian coordinates is determined by the following equation at each point:

$$\begin{cases} x_i = x - X \\ y_i = y - Y \\ z_i = z - Z \end{cases}. \quad (1)$$

In Equation 1, ($X$, $Y$) are the distances between the two coordinates on the plane of *xoy*. These assumptions are obvious in Figure 1b. According to Figure 1b, the stress arising from each one of the point loads of $P_0$ and $P_i$ can be obtained through the coordinates of ($x$, $y$, $z$) and ($x_i$, $y_i$, $z_i$) respectively.

If both of the point loads are applied simultaneously, the stress created at the point A will be equal to the sum of the stress caused by each one of them. When n point loads are applied to a rectangular surface, the obtained stress is equal to the sum of the stresses caused by all the point loads applying to the surface.

### 2.1. Boussinesq point load extension

In 1885, Boussinesq solved the problem of calculating stress distribution within a homogeneous, elastic, and isotropic semi-infinite material due to a point load applied to it. In this problem, the stress equation will be as follows at an arbitrary point of *A* [2]:

$$\sigma_z = \frac{3Pz^3}{2\pi}\int_{-b}^{b}\int_{-a}^{a}\frac{1}{\left(X^2+Y^2+z^2\right)^{5/2}}dXdY \tag{2}$$

$$\Rightarrow \sigma_z = qa,$$

where:

$\sigma_z$ – the vertical stress at the point *A* with the coordinates of (*x*, *y*, *z*), *P* is the value of point load and *l* is the distance between the coordinates origin and point *A*.

#### 2.1.1. Boussinesq one-dimensional rectangular extended point load ($x = 0, y = 0, z \neq 0$)

In the analysis of one-dimensional stress distribution, the coordinates of (*x*, *y*) were set to be zero to calculate the stress on the z-axis only. According to Figure 1b, and Equation 2, the stress at the point of *A* arose from the point loads of $P_0$ and $P_i$ can be calculated as follows:

$$\left(x,y,z\right):\sigma_{z0} = \frac{3P_0}{2\pi}\cdot\frac{z^3}{l_0^5} = \frac{3P_0}{2\pi}\cdot\frac{z^3}{\left(x^2+y^2+z^2\right)^{5/2}}; \tag{3}$$

$$\left(x_i,y_i,z_i\right):\sigma_{zi} = \frac{3P_i}{2\pi}\cdot\frac{z^3}{l_i^5} = \frac{3P_i}{2\pi}\cdot\frac{z^3}{\left(x_i^2+y_i^2+z_i^2\right)^{5/2}}. \tag{4}$$

Considering Equation 1, the relationship between *P*-any point load applied to the rectangular area- and the global coordinate is expressed generally as follows:

$$\sigma_z = \frac{3P}{2\pi}\cdot\frac{z^3}{\left(\left(x-X\right)^2+\left(y-Y\right)^2+z^2\right)^{5/2}}. \tag{5}$$

The differential form of Equation 5 can be obtained as follows:

$$d\sigma_z = \frac{3dP}{2\pi}\cdot\frac{z^3}{\left(\left(x-X\right)^2+\left(y-Y\right)^2+z^2\right)^{5/2}}. \tag{6}$$

Setting Equation 6 to be in accordance with the one-dimensional analysis assumptions and integrating it over the supposed rectangular area will result in an equation describing the stress along the *z*-axis (Equation 8).

$$\sigma_z = \frac{3Pz^3}{2\pi}\int_{-b}^{b}\int_{-a}^{a}\frac{1}{\left(X^2+Y^2+z^2\right)^{5/2}}dXdY \tag{7}$$

$$\Rightarrow \sigma_z = qa\frac{z^3}{\pi}K, \tag{8}$$

where:

$\sigma_z$ – the one-dimensional stress along the *z*-axis;

*a* – half the length of the assumed rectangle;

*z* – the coordinate of the point at which the stress is been calculated;

*K* – the influence factor depended on the rectangle dimensions along with *z* coordinate (Equation 8).

$$K = \frac{1}{250}b\sum_{i=0}^{499}\frac{3J+2a^2+3z^2}{\left(\left(J+z^2\right)^2\left(J+a^2+z^2\right)\right)^{3/2}}; \tag{9}$$

$$J = \left(-b+\frac{1}{250}\left(i+\frac{1}{2}\right)b\right)^2.$$

The Equation 8 is named B-1DREPL – that stands for "Boussinesq One-Dimensional Rectangular Extended Point Load" – which the resultant diagram of stress concentration is presented in Figure 4 that shows a decreasing trend along with *z*-axis.

#### 2.1.2. Boussinesq two-dimensional rectangular extended point load ($x \neq 0, y = 0, z \neq 0$)

As it is apparent, two-dimensional means involving two coordinates in which here is (*x*, *z*). According to Figure 1b cutting the loading space on the *x*-direction provides the plane of *xoz* which is discussed in this section. Analytically, setting y coordinate zero in Equation 5 will satisfy the theoretical assumptions. Considering these conditions, Equation 5 will be as follows:

$$\sigma_z = \frac{3Pz^3}{2\pi}\int_{-b}^{b}\int_{-a}^{a}\frac{1}{\left(\left(x-X\right)^2+Y^2+z^2\right)^{5/2}}dXdY. \tag{10}$$

After solving the integration of Equation (10), the answer named B-2DREPL – that stands for "Boussinesq Two-Dimensional Rectangular Extended Point Load" – will be as follows which describes the two-dimensional stress occurred on the plane of *xoz*:

$$\Rightarrow \sigma_z = qz^3\frac{b}{500\pi}\left(A+B\right), \tag{11}$$

where:

$\sigma_z$ – the two-dimensional stress on the plane *xoz*;

*b* – half the width of the assumed rectangle;

*z* – the coordinate of the point in which the stress is been calculated at;

*A* and *B* – the influence factors depended on the rectangle dimensions along with coordinates of (*x*, *z*) (Equation 12 and 13):

Equation 12

$$A = \frac{1}{3\cdot 250}\sum_{i=0}^{499}\frac{2a^3-6a^2x+3a\left(J+2x^2+z^2\right)-3\left(Jx-2x^3-3xz^2\right)}{\left(\left(a-x\right)^2+J+z^2\right)^{3/2}\left(J+z^2\right)^2}$$

Equation 13

$$B = \frac{1}{3\cdot 250}\sum_{i=0}^{499}\frac{2a^3-6a^2x+3a\left(J+2x^2+z^2\right)+3\left(Jx-2x^3-3xz^2\right)}{\left(\left(a-x\right)^2+J+z^2\right)^{3/2}\left(J+z^2\right)^2}$$

$$J=\left(-b+\frac{1}{250}\left(i+\frac{1}{2}\right)b\right)^2.$$

The resultant diagram of stress concentration counters is presented in Figure 5 that is established using the generated Matlab codes..

### 2.2. Westergaard point load extension

In 1938, Westergaard provided an elastic solution for the problem of calculating stress distribution within a non-isotropic material due to a point load applied to it. In Equation 14, the Poisson ratio was utilized so as to express the method of calculation [9]:

$$\sigma_z=\frac{Q}{z^2}\cdot\frac{\frac{1}{2\pi}\sqrt{\frac{1-2\upsilon}{2(1-\upsilon)}}}{\left(\left(\frac{1-2\upsilon}{2(1-\upsilon)}\right)+\left(\frac{r}{z}\right)^2\right)^{3/2}},\tag{14}$$

where:

$\sigma_z$ – the vertical stress at the point $A$ with the coordinates of ($x$, $y$, $z$);

$Q$ – the amount of point load;

$r$ – the distance from the origin of the coordinate to the projection of point $A$ on the plane of $XOY$;

$\upsilon$ – the Poisson ratio of the object which is being loaded.

#### 2.2.1. Westergaard one-dimensional rectangular extended point load ($x = 0, y = 0, z \neq 0$)

Similar to the solution provided for the Boussinesq point load extension, in the analysis of one-dimensional stress distribution using Westergaard point load, the coordinates of ($x$, $y$) were set to be zero to calculate the stress along the $z$-axis. According to Figure 1b, and Equation 14, the stress occurred at the point of $A$ due to point loads of $P_0$ and $P_i$ will be as follows:

$$(x,y,z):\sigma_{z0}=\frac{P_0\eta_c}{2\pi z^2}\cdot\frac{1}{\left(\eta_c^2+\frac{x^2+y^2}{z^2}\right)^{3/2}};\tag{15}$$

$$(x_i,y_i,z_i):\sigma_{zi}=\frac{P_i\eta_c}{2\pi z^2}\cdot\frac{1}{\left(\eta_c^2+\frac{x_i^2+y_i^2}{z^2}\right)^{3/2}};\tag{16}$$

$$\eta_c=\sqrt{\frac{1-2\upsilon}{2(1-\upsilon_c)}}.$$

Considering Equation 1, the relationship between $P$ – any point load applied to the rectangular area – and the global coordinate can be stated as followed generally.

$$\sigma_z=\frac{q\eta_c}{2\pi z^2}\int_{-b}^{b}\int_{-a}^{a}\frac{1}{\left(\eta_c^2+\frac{X^2+Y^2}{z^2}\right)^{3/2}}dXdY$$
$$\Rightarrow\sigma_z=qa\frac{\eta_c z}{\pi}K,\ \eta_c=\sqrt{\frac{1-2\upsilon_c}{2(1-\upsilon_c)}}.\tag{17}$$

Therefore, the differential form of the Equation 17 is calculated as follows:

$$d\sigma_z=\frac{dP\eta_c}{2\pi z^2}\cdot\frac{1}{\left(\eta_c^2+\frac{(x-X)^2+(y-Y)^2}{z^2}\right)^{3/2}}.\tag{18}$$

Integrating Equation 18 over the mentioned rectangular area (Fig. 1b) provides the final equation calculating the one-dimensional stress distribution along the $z$-axis which is perpendicular to the loading face.

$$\sigma_z=\frac{q\eta_c}{2\pi z^2}\int_{-b}^{b}\int_{-a}^{a}\frac{1}{\left(\eta_c^2+\frac{X^2+Y^2}{z^2}\right)^{3/2}}dXdY;\tag{19}$$

$$\Rightarrow\sigma_z=qa\frac{\eta_c z}{\pi}K,\ \eta_c=\sqrt{\frac{1-2\upsilon_c}{2(1-\upsilon_c)}};\tag{20}$$

$$K=\frac{1}{250}b\sum_{i=0}^{499}\frac{1}{\left(\eta_c^2z^2+J\right)\sqrt{a^2+\eta_c^2z^2+J}}.\tag{21}$$

$$J=\left(-b+\frac{1}{250}\left(i+\frac{1}{2}\right)b\right)^2.$$

The Equation 19 is named W-1DREPL – that stands for "Westergaard One-Dimensional Rectangular Extended Point Load" – where $\sigma_z$, $q$, $a$, $z$ and $\upsilon_c$ are the one-dimensional stress along the $z$-axis, the initial stress applied to the loading face, half the length of the rectangular loading face, the coordinate of the point on the $z$-axis in which the stress is been calculated, and the Poisson ratio of the material that is under loading respectively. $K$ is the influence factor depended on the rectangle dimensions, coordinate and Poisson ratio (Equation 21). The resultant diagram of stress concentration is shown in Figure 4.

#### 2.2.2. Westergaard two-dimensional rectangular extended point load ($x \neq 0, y = 0, z \neq 0$)

In the two-dimensional stress distribution analysis, the coordinate of $y$ is set to be zero to calculate the stress distribution on the plane of xoz that is perpendicular to the loading area. Considering these assumptions in Equation 1 and integrating over the rectangular area will provide the desired response.

$$\sigma_z=\frac{q\eta_c}{2\pi z^2}\int_{-b}^{b}\int_{-a}^{a}\frac{1}{\left(\eta_c^2+\frac{(x-X)^2+Y^2}{z^2}\right)^{3/2}}dXdY;\tag{22}$$

$$\Rightarrow\sigma_z=q\eta_c\frac{b}{500\pi z^2}(A+B),\ \eta_c=\sqrt{\frac{1-2\upsilon_c}{2(1-\upsilon_c)}}.\tag{23}$$

The Equation 23 is named W-2DRDPL – that stands for "Westergaard Two-Dimensional Rectangular Extended Point Load" – where $\sigma_z$, $q$, $b$ and $\upsilon_c$ are two-dimensional stress distribution on the plane $xoz$, the initial stress applied to the rectangular area, half the width of the loading face which is an arbitrary rectangle, and the Poisson ratio of the material that is being loaded respectively. $A$ and $B$ are equations depended on the rectangle dimensions, coordinates of $x$ and

$z$, and the Poisson ratio (Equation 24 and 25). The resultant diagram of stress concentration counters is presented in Figure 5 that is established using the generated Matlab codes..

$$A=\frac{1}{250}b\sum_{i=0}^{499}\frac{(a-x)z^3}{\left(\eta_c^2z^2+J\right)\sqrt{(a-x)^2+\eta_c^2z^2+J}}; \quad (24)$$

$$B=\frac{1}{250}b\sum_{i=0}^{499}\frac{(a+x)z^3}{\left(\eta_c^2z^2+J\right)\sqrt{(-a-x)^2+\eta_c^2z^2+J}}; \quad (25)$$

$$J=\left(-b+\frac{1}{250}\left(i+\frac{1}{2}\right)b\right)^2.$$

## 3. Numerical method

The finite element method is used to implement the numerical solution to the problem proposed in this study. The finite element method is a numerical method for solving problems of engineering and mathematical physics. Typical problem areas of interest in engineering and mathematical physics that are solvable by the use of the finite element method including structural analysis, heat transfer, fluid flow, mass transport, and electromagnetic potential. The 3D Abaqus finite element software package is been adopted in this study.

### 3.1. Numerical model construction

To approach the target described in this paper, a numerical model was constructed in the Abaqus software in 3D space. In order to construct the numerical model, an arbitrary cube with dimensions of 1×1×1.5 m was built. Subsequently, a rectangular loading area with dimensions of 0.4×0.2 m was considered at the center of the model (Fig. 2). Indeed, the model itself cannot provide the conception of being semi-infinite, but in comparison to the loading area, the whole model can satisfy the assumptions. The boundary condition of ENCASTRE is considered for the lower plane of the model in which all the movements and rotations are zero ($U_1 = U_2 = U_3 = UR_1 = UR_2 = UR_3 = 0$) (Fig. 2a).

For meshing the model, the standard eight-node linear cubic elements (C3D8R) were adopted with dimensions of 0.03×0.03×0.03 m and 0.02×0.02×0.03 m at the loading area (Fig. 2a).

According to (Fig. 2a), the uniform load was applied to the assumed rectangular area with an amount of 20 MPa. In fact, the stress concentration is calculated inside the material so the amount of load does not matter.

### 3.2. Material properties used in this study

In numerical studies, one of the most important early steps is to input the initial data. These data should be carefully monitored. The materials used in the present study are provided from Tabriz Metro line-2 Project (Table 1).

To provide input data for the numerical software, concrete behavioral information is required. Accordingly, the compressive mechanical properties should be determined through either tests or predictive analytical models. Due to the lack of experimental information, the proposed analytical models were used. Here is a summary of formerly presented analytical models.

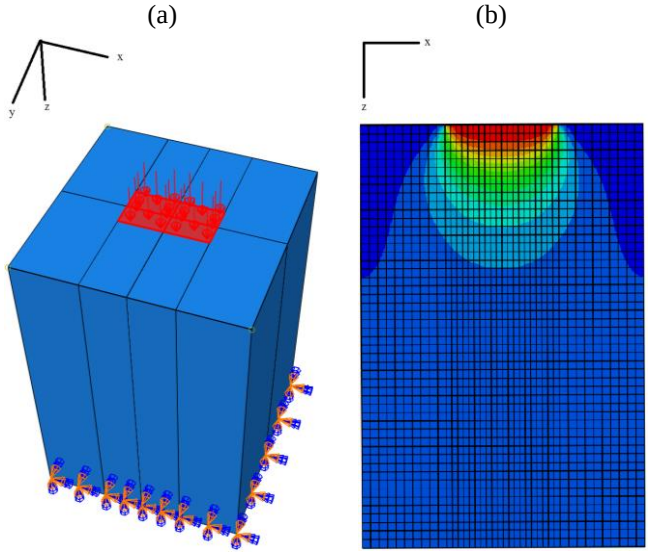


***Figure 2. Schematic of numerical model construction with the assumed boundary conditions (a); result of numerical study including two-dimensional stress distribution on the plane xoz (b)***

***Table 1. Mechanical properties of concrete used in the lining of Tabriz metro line-2 project***

| Mechanical property | Symbol | Value | Unit |
|---|---|---|---|
| 28-day uniaxial compressive strength | $f'_c$ | 40 | MPa |
| Young's modulus | $E$ | 30 | GPa |
| Poisson ratio | $\upsilon_c$ | 0.2 | – |
| Density | $\rho$ | 2500 | kg/m$^3$ |
| Rupture modulus | $f_r$ | 4.42 | MPa |

Hognestad introduced a new equation for the stress-strain curve by changing the Ritter's parabola equation. This equation is valid only in the elastic region until the ultimate stress (ultimate strength of the concrete) and provides an acceptable estimate of the behavior of the concrete in this area. Hognestad assumed the behavior of the residual region as a linear one and expressed its value of about 85% of the ultimate strength [10]. Kent and Park provided an equation for the concrete stress-strain curve and tried to explain the post-peak behavior more comprehensively by generalizing the Hognestad equation. In this model, the post-peak branch was assumed to be a straight line, whose slope is a function of concrete strength [11].

Popovics provided an equation to estimate the stress-strain behavior of concrete independently. The main advantage of this equation is controlling the pre-peak and post-peak behavior with three parameters of $f'_c$, $\varepsilon_0$ and $E_c$ (the ultimate strength, the strain corresponds to the ultimate strength and elastic modulus respectively). The Popovics equation provides a very good response for ordinary concretes ($f'_c < 55$ MPa). However, for high strength concrete, there is a lack of control over the slope of the post-peak area [12].

Tsai presented the generalized equation of the Popovics model. This equation has better control over the post-peak behavior of the stress-strain curve [13]. This model provides two parameters to control the slope and behavior of the post-peak branch [14]. A summary of all the predicting analytical models is presented in Table 2. A comparison of the models is shown in Figure 3a. Since the concrete used in this study has a strength of less than 55 MPa, the Popovics model was chosen as the stress-strain behavior under the compressive loading.

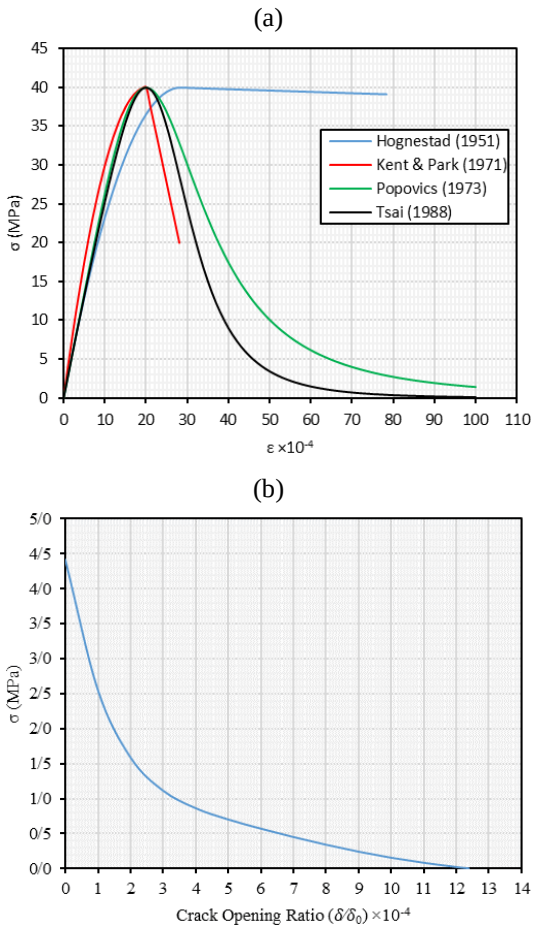


***Figure 3. A comparison of predicting analytical models for compressive behavior (a); the relationship between tensile stress and the ratio of instantaneous opening to the ultimate opening based on the Hordijk equation (b)***

Tensile strength and tensile behavior of concrete structures are very important. In most cases, cracks and ruptures in the concrete blocks are associated with this characteristic. To simulate the tensile behavior of the concrete used in the present study, the Hordijk model was used with the following Equation [15]:

$$\frac{\sigma}{f_t}=\left\{1+\left(c_1\frac{\delta}{\delta_0}\right)\right\}\exp\left(c_1\frac{\delta}{\delta_0}\right)-\frac{\delta}{\delta_0}\left(1+c_1^3\right)\exp\left(-c_2\right). \quad (26)$$

That $\sigma$, $f_t$, $\delta$ and $\delta_0$ are tensile stress, tensile strength, crack Instantaneous opening, and crack ultimate opening respectively. The value of $\delta_0$ is 140 and 160 μm for lightweight and ordinary concrete respectively. The value of $c_1$ and $c_2$ are 1 and 5.64 for lightweight concrete and 3 and 6.93 for ordinary one [15]. The properties of ordinary concrete were used in this study and the diagram of tensile behavior is presented in Figure 3b.

The resultant diagrams of the numerical study of the one-dimensional and two-dimensional stress distribution within the material being loaded are shown in the next section.

## 4. Discussion

According to the assumptions of the Boussinesq point load equation, the mechanical properties of the material being loaded are not considered and subsequently, the resultant stress distribution calculated within the material depends on the coordinates merely. Therefore, the resultant equations presented in this study due to integration over a rectangular area depends on the coordinates similarly. However, the Westergaard point load equation responds based on coordinates and Poisson ratio of the material. Hence the properties of the material are somehow involved in the calculations and subsequently, it is assumed in the equations newly presented in this paper due to a rectangular loading area. Accordingly, in the analysis of one-dimensional stress distribution, B-1DREPL depends on the coordinate of $z$ merely in which the stress is calculated. On the other side, W-1DREPL depends on both the coordinate of $z$ and the Poisson ratio. In the same way, in the analysis of two-dimensional stress distribution, B-2DREPL depends on the coordinates of ($x$, $z$), and W-2DREPL depends on the coordinates of ($x$, $z$) and Poisson ratio.

According to the results of one-dimensional stress distribution analysis (Fig. 4), the intensity of stress concentration decreases sharply about 90% in a distance of 50 cm out of 150 cm which is about 33% of the material height. The intensity of stress concentration remains constant and low from the point $z$ = 50 cm to the end that is about 5% of the initial amount. According to Figure 4, the trend of stress concentration variation in three methods of B-1DREPL, W-1DREPl, and the numerical method is almost the same. More precisely, the answer obtained from B-1DREPL is closer to the numerical solution than the answer provided by W-1DREPL from $z$ = 0 cm to $z$ = 50 cm. However, the two analytical methods get closer together from $z$ = 50 cm to the $z$ = 150 cm.

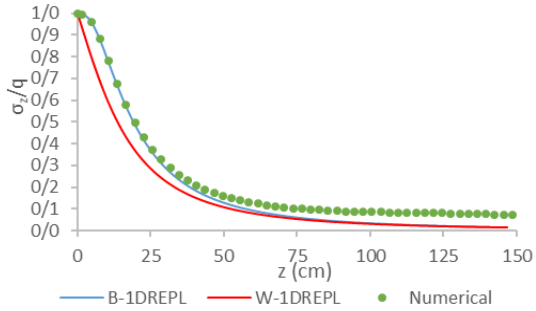


***Figure 4. The results of one-dimensional stress concentration distribution analysis***

As mentioned before, to provide graphical results of the two-dimensional stress distribution analysis, MATLAB codes were generalized for both the B-2DREPL and the W-2DREPL. Accordingly, obtained Pressure Bulbs are illustrated in Figure 5 that represents the stress concentration intensity on the plane *xoz* perpendicular to the loading face in three different methods.

As shown in Figure 5, the highest stress concentration is immediately below the loading face and it decreases gradually by getting farther from that face. Each method provides its counterplot but generally, they are the same. To have a deep view about the differences between the results of the three used methods, 5 reference points of *A*, *B*, *C*, *D*, and *E* were assumed on the plane of *xoz* where the counterplot of stress concentration distribution was drawn (Fig. 6a).

Point *A* is immediately under the loading face, point *B* is at the left side, point *C* is at the center, point *D* is at the right side, and *E* is the farthest point in comparison to the loading face. Accordingly, the Stress Concentration Difference (SCD) between the numerical method and B-2DREPL (SCDNB) and also between the numerical method and W-2DREPL (SCDNW) is illustrated in Figure 6b.

***Table 2. The predicting analytical equations for a compressive stress-strain diagram***

| Equation | Description | Reference |
|---|---|---|
| $f_c = f_c''\left[\frac{2\varepsilon_c}{\varepsilon_{c0}} - \left(\frac{\varepsilon_c}{\varepsilon_{c0}}\right)^2\right]$; $\varepsilon_{c0} = \frac{2f_c'}{E_c}$, $f_c'' = 0.85f'$. | $E_c$, $\varepsilon_{c0}$, $\varepsilon_c$, $f'_c$ and $f_c$ are elastic modulus, strain corresponds to the concrete strength, instantaneous strain, concrete strength, and instantaneous stress respectively. | Hognestad, 1951 [10] |
| $f_c = f_c'\left[\frac{2\varepsilon_c}{\varepsilon_{c0}} - \left(\frac{\varepsilon_c}{\varepsilon_{c0}}\right)^2\right]$; $f_c = f_c'\left[1 - Z\left(\varepsilon_c - \varepsilon_{c0}\right)\right]$; $Z = \frac{0.5}{\varepsilon_{50u} - \varepsilon_{c0}}$; $\varepsilon_{50u} = \frac{3 + 0.29f_c}{145f_c - 1000}$ ($f'_c$ in MPa); $\varepsilon_{50u} = \frac{3 + 0.002f_c'}{f_c' - 1000}$ ($f'_c$ in Psi). | $E_c$, $\varepsilon_{c0}$, $\varepsilon_c$, $f'_c$ and $f_c$ are elastic modulus, strain corresponds to the concrete strength, concrete strength, and stress respectively. $E_{50u}$ is the strain corresponds to stress equivalent to 50% of the concrete strength. | Kent and Park, 1971 [11] |
| $\frac{f_c}{f_c'} = \frac{n\left(\frac{\varepsilon_c}{\varepsilon_{c0}}\right)}{(n-1) + \left(\frac{\varepsilon_c}{\varepsilon_{c0}}\right)^n}$; $n = 1.0 + 0.4 \cdot 10^{-3} \cdot f'$ (Psi). | $\varepsilon_{c0}$, $\varepsilon_c$, $f'_c$ and $f_c$ are strain corresponds to the concrete strength, instantaneous strain, concrete strength, and instantaneous stress respectively. $n$ is the approximation function based on the compressive strength of the concrete. | Popovics, 1973 [12] |
| $y = \frac{mx}{1 + \left(m - \frac{n}{n-1}\right)x + \frac{x^n}{n-1}}$; $y = \frac{f_c}{f_c'}$, $x = \frac{\varepsilon}{\varepsilon_c}$ $m = 1 + \frac{1.79}{f'(MPa)}$ ; $n = \frac{f'(MPa)}{6.68} - 1.85 > 1$ $m = 1 + \frac{1.79}{f'(MPa)}$; $n = \frac{f'(MPa)}{6.68} - 1.85 > 1$; $m = 1 + \frac{2600}{f'(Psi)}$; $n = \frac{f_c'(Psi)}{970} - 1.85 > 1$. | $y$ is the ratio of instantaneous stress to the ultimate strength; $x$ is the ratio of instantaneous strain to the strain at $y = 1$ and $n$ is the controlling factor over the post-peak region slope. | Tsai, 1987 [13] |

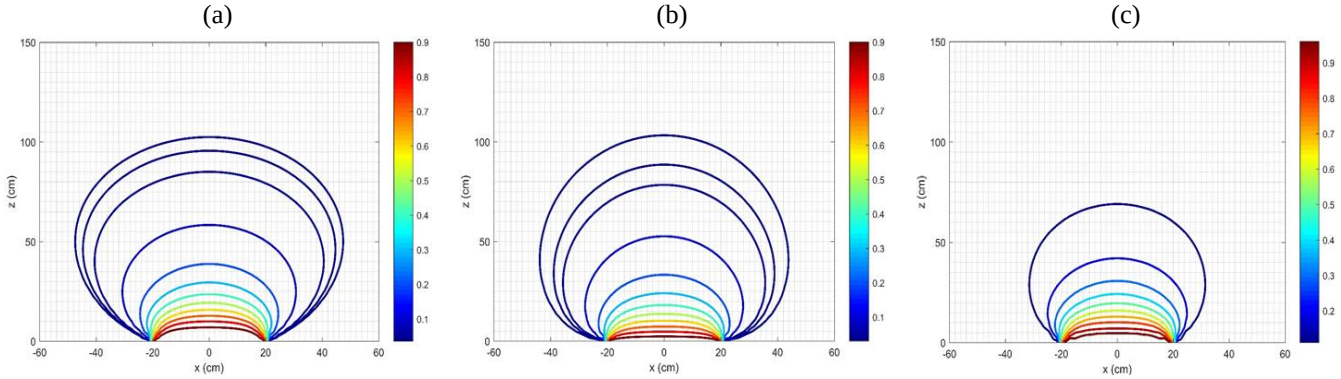


***Figure 5. The results of two-dimensional stress concentration distribution analysis: (a) B-2DREPL; (b) W-2DREPL; (c) numerical***

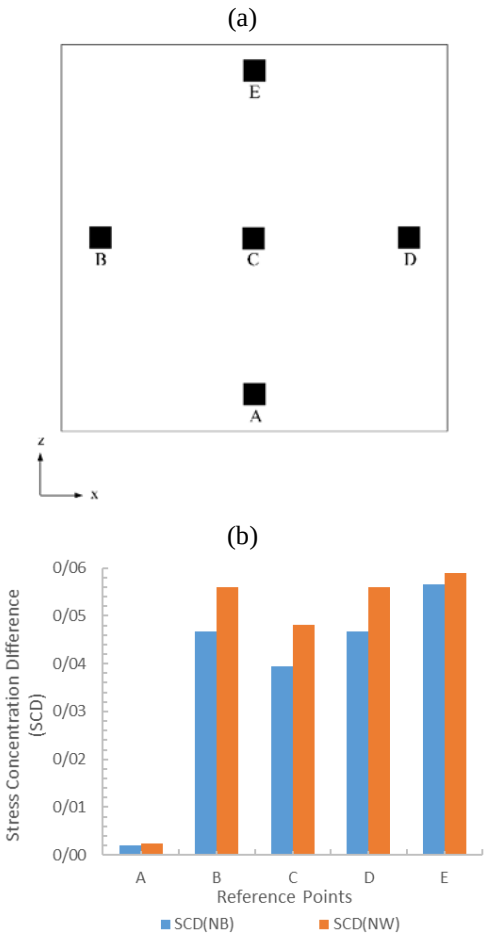


***Figure 6. Selected reference points on the plane xoz (a); results of SCD study at the reference points (b)***

According to Figure 6b, SCD increases from point *A* to point *E* generally and the maximum SCD is 0.06 out of 1 at point *E* that is acceptable so that this claim is also proved in one-dimensional analysis in Figure 4. SCDNB and SCDNW are almost equal and their amount is less than 0.001 out of 1 which clarifies the accuracy and validity of the analytical study. From point *B* to point *E*, the amount of SCDNB is less than SCDNW. Therefore, B-2DREPL is closer to the numerical method than W-2DREPL but it doesn't mean that W-2DREPL is unusable.

## 5. Conclusions

This paper focuses on the calculation of stress distribution within an elastic semi-infinite material due to an arbitrary rectangular uniform loading which was studied in both the analytical and the numerical methods. In the analytical section, well-known Boussinesq and Westergaard point load equations were extended to study the stress distribution within an elastic semi-infinite material due to an arbitrary rectangular uniform loading. Accordingly, four new equations were represented in this paper to describe the stress distribution one-dimensionally and two-dimensionally. Consequently, a numerical model was constructed using Finite Element based Abaqus software.

According to the results, numerical and analytical answers to the problem of rectangular loading are highly close together that confirms the accuracy and validity of the newly presented equations. in one-dimensional stress analysis, it was realized that the stress concentration decreases sharply up to 33% of the material height, and from that point onwards, it remains almost constant and low. Therefore, two equations of B-1DREPL and W-1DREPL were introduced to calculate the one-dimensional stress distribution on the z-axis perpendicular to the loading face. In two-dimensional stress analysis, two equations of B-2DREPL and W-2DREPL were presented. However, because of their complexity, MATLAB codes were generalized to simplify the process of calculating.

To have a deep view of the differences between the three proposed methods, five reference points were assumed on the plane of *xoz* perpendicular to the loading face. Consequently, a parameter of SCD was defined as Stress Concentration Difference between the analytical and numerical results. According to the obtained results, SCD increases as the reference point gets farther from the loading face. However, SCDNB is less than SCDNW generally. The newly presented equations in this paper can contribute to solving the problems engaged with the loading process in mining, rock mechanics, geotechnics, and civil.

## Acknowledgements

The authors highly appreciate Tabriz Metro Line-2 project management for providing initial data. The authors declare this research did not receive any specific grant from funding agencies in the public, commercial, or not-for-profit sectors.

## References

[1] Lama, B., & Clapeyron, G. (2009). Mémoire sur l'équilibre intérieur des corps solides homogènes. *Journal für die Reine und Angewandte Mathematik, 7*(391-423), 33. https://doi.org/10.1515/crll.1831.7.145

[2] Boussinesq, J. (1885). *Application des potentiels à l'étude de l'équilibre et du mouvement des solides élastiques: Principalement au calcul des déformations et des pressions que produisent, dans ces solides, des efforts quelconques exercés sur une petite partie de leur surface ou de leur intérieur: mémoire suivi de notes étendues sur divers points de physique, mathematique et d'analyse* (pp. 1842-1929). Paris, France: Gauthier-Villars.

[3] Love, A.E.H. (1929). IX. The stress produced in a semi-infinite solid by pressure on part of the boundary. *Philosophical Transactions of the Royal Society of London. Series A, Containing Papers of a Mathematical or Physical Character*, *228*(659-669), 377-420. https://doi.org/10.1098/rsta.1929.0009

[4] Terazawa, K.I. (1916). On the elastic equilibrium of a semi-infinite solid under given boundary conditions. *Journal of the College of Science*, 14-24.

[5] Sadd, M.H. (2009). *Elasticity: Theory, applications, and numerics*. Cambridge, United States: Academic Press, 600 p.

[6] Newmark, N.M. (1942). *Influence charts for computation of stresses in elastic foundations*. Urbana, United States: University of Illinois, 40 p.

[7] Fadum, R.E. (1941). *Influence values for vertical stresses in a semi-infinite elastic solid due to surface loads*. Cambridge, United States: Harvard University, 19 p.

[8] Steinbrenner, W. (1934). *Tafeln zur setzungsberechnung*. Die StraBe.

[9] Westergaard, H. (1939). *A problem of elasticity suggested by a problem in soil mechanics: Soft material reinforced by numerous strong horizontal sheets* (pp. 120-130). Cambridge, United States: Harvard University.

[10] Hognestad, E. (1951). *Study of combined bending and axial load in reinforced concrete members*. Urbana, United States: University of Illinois, 134 p.

[11] Kent, D.C., & Park, R. (1971). Flexural members with confined concrete. *Journal of the Structural Division, 97*(7), 1969-1990. https://doi.org/10.1061/JSDEAG.0002957

[12] Popovics, S. (1973). A numerical approach to the complete stress-strain curve of concrete. *Cement and Concrete Research, 3*(5), 583-599. https://doi.org/10.1016/0008-8846(73)90096-3

[13] Tsai, W.T. (1988). Uniaxial compressional stress-strain relation of concrete. *Journal of Structural Engineering, 114*(9), 2133-2136. https://doi.org/10.1061/(ASCE)0733-9445(1988)114:9(2133)

[14] Reddiar, M.K.M. (2010). *Stress-strain model of unconfined and confined concrete and stress-block parameters*. PhD Thesis. College Station, United States: Texas A&M University.

[15] Cornelissen, H., Hordijk, D., & Reinhardt, H. (1986). Experimental determination of crack softening characteristics of normal weight and lightweight. *Heron, 31*(2), 45-46.

**Аналітичне і чисельне дослідження одновимірного та двовимірного розподілу напружень у пружному напівнескінченному матеріалі під дією довільного прямокутного рівномірного навантаження**

Ф.Ш. Малекі, Х. Чакері, С. Чехрегані, Х.А. Соула

**Мета.** Дослідження одновимірного та двовимірного розподілів внутрішніх напружень у пружному напівнескінченному матеріалі під дією зовнішнього довільного прямокутно-квадратного навантаження.

**Методика.** У даній статті використовуються як аналітичний, так і чисельний методи. В аналітичному дослідженні застосовуються рівняння точкового навантаження Бусінеска та Вестергаарда. Поширюючи ці рівняння на прямокутну площу навантаження, вводяться чотири нових рівняння. За допомогою скінченно-елементного програмного забезпечення Abaqus чисельне дослідження виконується в 3D просторі.

**Результати.** Встановлено, що відповіді введених рівнянь добре узгоджуються з числовими результатами, проте результат розширеного рівняння точкового навантаження Бусінеска ближче до відповіді, отриманої чисельним методом. Встановлено, що при одномірному аналізі напружень їх концентрація стрімко знижується до 33% висоти матеріалу, і з цього моменту вона залишається майже постійною та низькою. Визначено, що параметр SCD може бути представлений як різниця концентрації напруження між аналітичними та чисельними результатами. Згідно з отриманими результатами, SCD збільшується в міру видалення контрольної точки від поверхні, що навантажується.

**Наукова новизна.** Вперше отримано чотири нові рівняння, що описують одновимірний і двовимірний розподіл напружень під дією зовнішнього навантаження.

**Практична значимість.** Наведені рівняння можуть забезпечити простий і зручний спосіб розв'язувати задачі прямокутного навантаження у багатьох випадках, таких як фундамент, цивільні та гірничі проєкти. У цьому дослідженні використовується початкова інформація про конкретні ділянки проєкту другої лінії Тебрізського метро.

***Ключові слова:*** *розподіл напружень, прямокутник, напівнескінченний, Бусінеск, Вестергаард*